Title

Enhanced Isomer Population via Direct Irradiation of Solid-Density Targets Using a Compact Laser-Plasma Accelerator

Authors

Jacob, Robert E

Tannous, Speero M

Bernstein, Lee A

et al.

Peer reviewed

Enhanced isomer population via direct irradiation of solid-density targets using a compact laser-plasma accelerator

Robert E. Jacob,[1, 2] Speero M. Tannous,[1] Lee A. Bernstein,[1, 2] Joshua Brown,[1] Tobias Ostermayr,[2] Qiang Chen,[2] Dieter H G. Schneider,[3] Carl B. Schroeder,[1, 2] Jeroen van Tilborg,[2] Eric H. Esarey,[2] and Cameron G R. Geddes[2]

[1]*Department of Nuclear Engineering, University of California, Berkeley, CA 94720*
[2]*Lawrence Berkeley National Laboratory, Berkeley, CA 94720*
[3]*Lawrence Livermore National Laboratory, Livermore, CA 94550*
(Dated: December 21, 2024)

Excitation of long-lived states in bromine nuclei using a table-top laser-plasma accelerator providing pulsed (<100 fs) electron beams provided a sensitive probe of gamma strength and level densities in the nuclear quasicontinuum, and may indicate angular momentum coupling through electron-nuclear interactions. Solid-density active $LaBr_3$ targets absorb real and virtual photons up to 35 ± 2.5 MeV and de-excite through gamma cascade into different states. A factor of 4.354 ± 0.932 enhancement of the $^{80}Br^m/^{80}Br^g$ isomeric ratio was observed following electron irradiation, as compared to bremsstrahlung. Additional angular momentum transfer could possibly occur through nuclear-plasma or electron-nuclear interactions enabled by the ultra-short electron beam. Further investigation of these mechanisms could have far-reaching impact including decreased storage of long-term nuclear waste and an improved understanding of heavy element formation in astrophysical settings.

INTRODUCTION

Long-lived isomeric states in nuclei have a broad range of implications. They have long been believed to play a particularly important role in stellar nucleosynthesis [1], especially in the $A = 80$ mass region [2]. Most recently, there has been a renewed theoretical interest in the population of Astrophysical Isomers (aka "Astromers") [3], with experimental evidence for the population of Kr isomers via laser-induced plasma-nuclear processes [4]. The vast majority of the population mechanisms suggested for these states proceed through individual, discrete low-lying states. However, the far larger density of unresolved "quasicontinuum" states with a broader range of angular momentum at higher excitation energies could provide a far more efficient mechanism for isomeric state populations.

The lifetime of low-lying nuclear levels which could serve as "doorways" into isomeric states have relatively long lifetimes on the order of nanoseconds, leading to an excitation energy width on the order of μeV via the $\Delta E \Delta t \geq \hbar/2$ uncertainty relation. This means that fewer than 1 part in 10^{13} radiation quanta are capable of exciting these states in a $k_b T \approx 30$ keV plasma. In contrast, the exponentially higher density of nuclear states at several MeV, together with the increased likelihood that numerous final states will exist that have significant overlap with a given initial level, will lead to a significantly increased excitation width via Fermi's Golden Rule:

$$T(E_\gamma, E_x) = [< f|V(E_i - E_f)|i >]^2 \times \rho(E_f), \quad (1)$$

where $\rho(E_f)$ is the nuclear level density (NLD) at the final state energy and $V(E_i - E_f)$ represents the interaction between the initial and final states, which in the case of bound states is proportional to the γ-strength functions (γSF). Together, these concepts represent the density of potential nuclear states and the probability of transitions between them, as a function of energy and spin. Per Guttormsen et al.[5], for nuclei with $A \approx 50 - 240$, the NLD will be $10^3 - 10^7$ levels per MeV near the neutron separation energy (S_n), and there is significant evidence of enhanced γSF in stable Molybdenum nuclei from photoneutron emission [6, 7] at high energies and particle transfer at low energies [8]. These high NLDs and γSFs make nuclei in this mass region an attractive target for nuclear isomer excitation, mitigating the ultra-narrow energy window facing direct excitation of long-lived isomers.

In addition to direct photonuclear excitation, nuclear-plasma interactions (NPIs) may provide another enhancement for isomer excitation in high energy density plasma environments [9, 10]. Of particular interest to this experiment are nuclear excitation by electron transition (NEET) [11, 12] and nuclear excitation by electron capture (NEEC) [13]. The NEET process describes nuclear excitation via virtual photon exchange as a result of electronic de-excitation within a partially ionized atomic shell. In contrast, NEEC describes nuclear excitation via virtual photon exchange induced by atomic electron capture into a partially ionized atomic shell. These processes can be thought of as time-reversed bound internal conversion and internal conversion nuclear decay processes, respectively [9]. Additionally, photon absorption and inelastic scattering of electrons from nuclei are present in these environments and provide other pathways for nuclear excitation.

When utilized together the nuclear quasicontinuum and NPIs offer an exciting tool to explore indirect isomer population in nuclei. Nuclei excited to states within the quasicontinuum may be readily susceptible to energy

and spin modifications as a result of NPIs with low energy background photons and plasma electrons. These excited states will de-excite to either the ground state or isomeric states, with unknown feeding ratios. It follows that excited nuclei with better matched spin may preferentially de-excite into isomeric states. Traditional accelerators have yet to do demonstrate probing of NPIs in the quasicontinuum with femtosecond beams.

Laser-plasma accelerators (LPAs) can provide ultra-short, high-energy electron bunches on the order of 10's of femtoseconds at high repetition rates [14]. LPAs enable high-repetition rate probing of NPIs, allowing nuclear states to be excited and further modified within ultra-short timescales. The goal of this experiment is to explore the quasicontinuum as a pathway to the indirect population of long lived isomers in ^{79}Br nuclei and observe potential modifications to feeding ratios in the presence of NEEC and NEET interactions using a novel experimental platform. Results will help develop understanding of nuclear-plasma interactions for applications in nuclear waste management and astrophysical settings.

EXPERIMENTAL SETUP

The irradiation target consisted of a 1 cm right cylinder LaBr$_3$ scintillator crystal mounted to a photo-multiplier tube which served as an "active target". The crystal was both an activation target and decay radiation detector, calibrated with a known ^{137}Cs check source. The ^{79}Br nucleus has a J$^\pi = 9/2^+$ isomeric state, ^{79}Br^m, at 207.6 keV with a half-life of 4.85 seconds, which decays by emission of a 207.6 keV γ-ray with an absolute intensity, I_γ^{abs}, of 76%, supplemented by internal conversion [33]. Immediately following irradiation the PMT was biased and allowed to observe decay radiation for 20 seconds, after which the PMT was unbiased and another irradiation was performed. This process was repeated for many shots with stable beam conditions to allow for the collection of sufficient counting statistics. Following the cumulative irradiation period, the PMT was biased to collect longer-lifetime decay radiation. This was performed after both the bremsstrahlung photon and electron irradiation cases. Rest time was significantly longer than the longest expected half-life of 4.42 hours for the 85.84 keV isomeric state, ^{80}Br^m, in ^{80}Br [34].

Two unique source configurations were used, one for direct irradiation of the target with electrons and another for bremsstrahlung photon irradiation of the target, shown in Figures 1a and 1b. For photon irradiation, a 0.46 T dipole magnet is used to disperse the electron beam for energy selection with a movable bremsstrahlung converter. The converter consists of a 2 mm tall, 5 mm deep stainless steel bar. A 0.75 T bending dipole magnet was used to prevent electrons from

State	Half-life, $\tau_{1/2}$	Target Nuclei
^{80}Br^m	4.42 hrs	^{81}Br
^{80}Br^g	17.68 mins	^{81}Br
^{79}Br^m	4.85 s	^{81}Br, ^{79}Br
^{78}Br^{m*}	119.4 μs	^{79}Br
^{78}Br^g	6.45 mins	^{79}Br
^{77}Br^{m*}	4.28 mins	^{79}Br
^{77}Br^{g*}	57.04 hrs	^{79}Br

TABLE I: Unstable products from (γ, n), (γ, γ') reactions on natural Br, from ENDF [32]

* Not observed

reaching the active target by bending them into a low Z beam dump. Bremsstrahlung photons up to 35 ± 2.5 MeV excite the target into the nuclear quasicontinuum. For electron irradiation, the bremsstrahlung converter and secondary bending dipole were removed from the experiment, allowing 35 ± 2.5 MeV, <100 fs electron bunches to excite nuclei into the quasicontinuum and promote electron-nuclear interactions in the target.

This experiment was performed at the BELLA Hundred Terawatt Thomson laser system, located at Lawrence Berkeley National Laboratory in Berkeley, California [15, 16]. For this experiment, a 1.75 J, 40 fs laser pulse was focused to a waist size of 17 μm FWHM with a peak intensity of 7.25×10^{18} W/cm^2 in a high-density gas jet, which produces <100 fs electron beams through laser-plasma accelerator mechanisms [14]. Electron beams were diagnosed with a magnetic spectrometer placed after a dispersive dipole magnet. A movable LANEX sheet was imaged and the energy-spatial dispersion calculated using RADIA [17]. The electron spectrum is shown in Figure 1c. For calculations performed later, the electron beam charge is not necessary.

RESULTS AND DISCUSSION

The LaBr$_3$ crystal is manufactured with natural bromine which contains an abundance of 50.69% ^{79}Br, with the remainder composed of ^{81}Br [18]. Population of the ^{79}Br^m state occurs via the ^{79}Br$(\gamma, \gamma')^{79}$Br^m and ^{81}Br$(\gamma, 2n)^{79}$Br^m reaction pathways. Given the approximately equal proportion of ^{79}Br and ^{81}Br nuclei in the active target, we are unable to attribute experimental excitations of the ^{79}Br^m state to a particular parent nuclei. Meanwhile, the ^{80}Br^m and ^{80}Br^g states are primarily populated via the ^{81}Br(γ, n) reaction. A list of possible bromine states is given in Table I.

For each irradiation case, inter-shot spectra were summed to create a shot-integrated decay spectrum. An example time-series is shown in Figure 2. The ^{79}Br^m signal was observed near 207 keV with a calculated
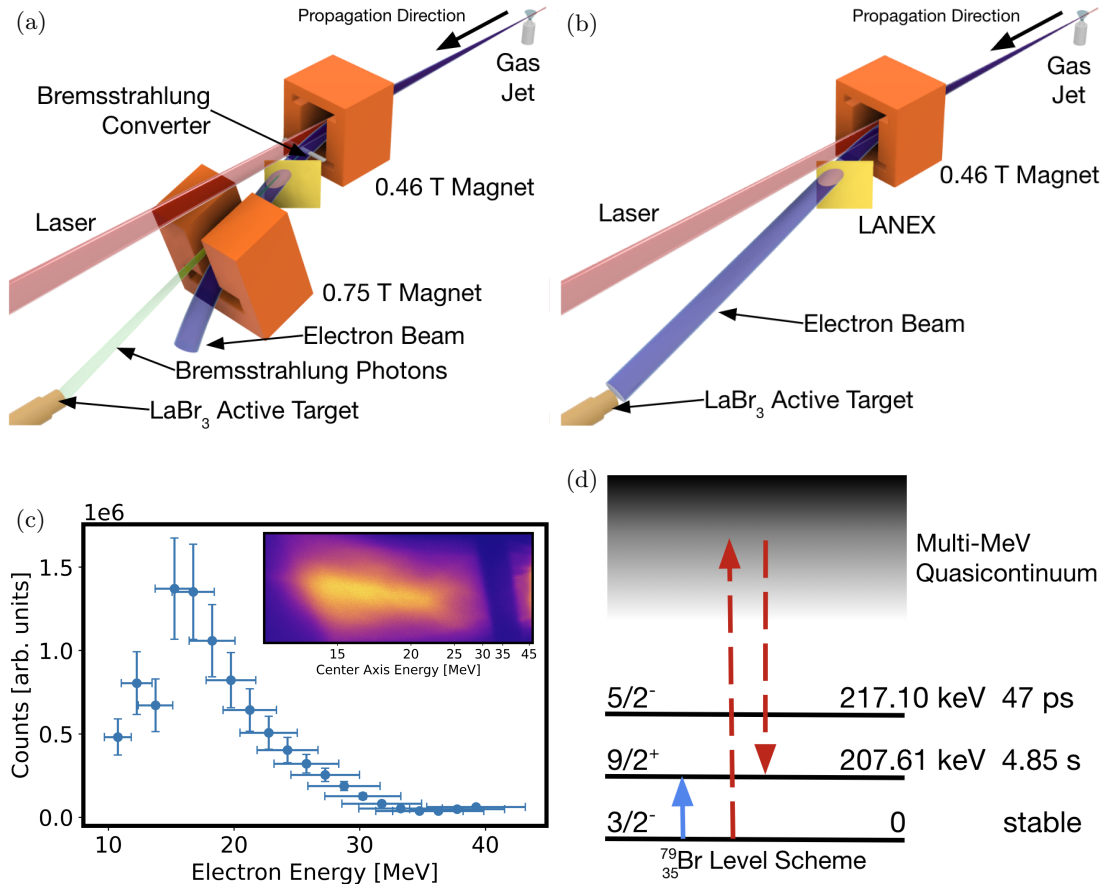
FIG. 1: (a) Experimental setup for bremsstrahlung photon irradiation, with the converter target and 0.75 T bending magnet shown. Diagnostic LANEX sheet was insertable after this first magnet, and could be moved out of the beam path to prevent unwanted electron scattering and bremsstrahlung generation. (b) Experimental setup for electron irradiation, with the converter and bending magnet removed. (c) Measured electron spectrum averaged over 100 shots, with inset of single-shot image showing the shadow from the bremsstrahlung converter. The slanted shadow is a result of the imaging geometry, with the LANEX screen normal at 45° to the laser axis. (d) Level diagram for ^{79}Br with a solid blue arrows indicating nearest-neighbor population of the isomeric state, and the dashed red arrows indicating excitation into the quasicontinuum complemented by subsequent nuclear-plasma interactions, shown in black, before de-excitation into the isomeric state.

$T_{1/2}^{exp} = 4.05 \pm 0.64$ seconds. From the post-irradiation spectra ^{80}Br^m decay was observed near 85 keV with a calculated $T_{1/2}^{exp} = 4.36 \pm 0.05$ hours. Additionally, the production of short-lived ^{80}Br^g and ^{78}Br^g nuclei was determined by fitting the post-irradiation e^-/e^+ and γ decay, $N_{Det}(t)$, between 0.5 and 2.3 MeV with Equation 4, where N_0^{80g}, λ_{80g}, N_0^{78g}, and λ_{78g} are fit while N_0^{80m} is fixed to the population determined from the post-irradiation spectrum, and λ_{80m} is fixed to the accepted value. Here N_0^i terms refer to the initial population of species i immediately following the irradiation period and λ_i the species' decay constant. The governing population equations are

$$N_{80g}(t) = \frac{\lambda_{80m}}{\lambda_{80g} - \lambda_{80m}} N_0^{80m} (e^{-\lambda_{80m}t} - e^{-\lambda_{80g}t}) + N_0^{80g} e^{-\lambda_{80g}t}, \quad (2)$$

$$N_{78g}(t) = N_0^{78g} e^{-\lambda_{78g}t}, \quad (3)$$

$$N_{Det}(t) = \Delta t \left(\eta_{80g} \lambda_{80g} N_{80g}(t) + \eta_{78g} \lambda_{78g} N_{78g}(t) \right) + C, \quad (4)$$

where Δt is the time bin width, C is a linear background term, and the η_i terms are detector response fractions calculated in FLUKA for the target geometry, respective
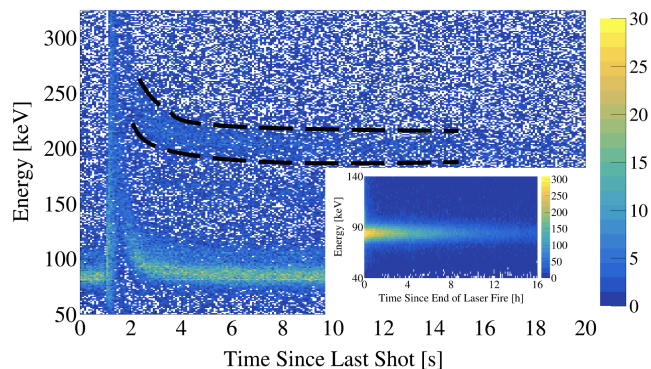
FIG. 2: Shot accumulated time-series data showing the accumulation and decay of the 207.6 keV ^{79}Br^m signal, highlighted with dashed lines. The curved detector response is a result of rapid biasing following an irradiation. The inset continuous time-series data shows the decay of the ^{80}Br^m state, over many hours after irradiation.

nuclei, and trimmed to the fit energy range [22]. Equation 2 describes the population evolution of ^{80}Br^g as a result of direct population and feeding from the ^{80}Br^m state. For ^{78}Br^g, single-state decay is the only source considered in Equation 3, given the 119.4 μs half-life of its isomeric state is too short to observe with the bias cycling of the detector [35]. For the bremsstrahlung case a normalized $\chi^2 = 1.000$ for $250 \leq t \leq 20,000$ seconds was achieved with fit $T^{80g}_{1/2} = 17.12 \pm 0.60$ min, $T^{78g}_{1/2} = 6.34 \pm 0.08$ min. For the electron case, a normalized $\chi^2 = 1.005$ was achieved for $50 \leq t \leq 12,500$ seconds and fit $T^{80g}_{1/2} = 18.24 \pm 0.67$ min, $T^{78g}_{1/2} = 5.82 \pm 0.07$ min. From these fits, a post-irradiation initial population for ^{80}Br^g and ^{78}Br^g was established.

For the isomeric transition (IT) peaks of ^{80}Br^m and ^{79}Br^m, time-binned projection slices were fitted with a Gaussian plus linear background fit and exponential decay corrected back to $t = 0$, then averaged in order to calculate an initial population. Photo-peak efficiencies for the characteristic gammas from ^{80}Br^m and ^{79}Br^m were calculated with FLUKA and weighted with their respective I^{abs}_γ, in the form $\eta_{peak} = \Sigma\eta_{geo}I^{abs}_\gamma + (1 - \Sigma I^{abs}_\gamma)$, to account for the internal conversion fraction with an assumed efficiency of 1 [22–24]. This adjustment yields a total population of ^{79}Br^m and the population of ^{80}Br^m following the irradiation period. Total populations for the ^{80}Br^m, ^{80}Br^g, and ^{78}Br^g states were found by calculating population and continuous decay over the duration of the experiment. Contributions from the decay of ^{80}Br^m to ^{80}Br^g were subtracted in order to determine direct ^{80}Br^g populations. The calculated Activations/Shot values are given in Table II with isomeric ratios (IRs) calculated for ^{79}Br^m/^{80}Br^m and ^{80}Br^m/^{80}Br^g, similar to the method presented in [20]. Table II includes statistical and systematic uncertainties attributed to the beta decay

	Bremsstrahlung	Electrons
^{79}Br^m [#/Shot]	28.97 ± 2.83	57.58 ± 1.75
^{80}Br^m [#/Shot]*	306.95 ± 17.95	744.22 ± 59.30
^{80}Br^g [#/Shot]*	1557.25 ± 195.10	809.53 ± 100.27
^{79}Br^m/^{80}Br^m	0.094 ± 0.011	0.077 ± 0.007
^{80}Br^m/^{80}Br^g	0.211 ± 0.033	0.919 ± 0.135

TABLE II: Activations/Shot for populated states with isomeric ratios

* These values are shot-averaged with decay corrected populations following the irradiation period.

detector response fitting (5%) and the decay correction (5%), where applicable. The presented IRs avoid systematic laser energy fluctuations, which have been measured with a FWHM < 3.3%[36].

TALYS 2.0 calculated cross sections for the ^{79}Br$(\gamma,\gamma')^{79}$Br^m, ^{81}Br$(\gamma,2n)^{79}$Br^m, ^{81}Br$(\gamma,n)^{80}$Br^m and ^{81}Br$(\gamma,n)^{80}$Br^g reactions were used with the FLUKA bremsstrahlung spectrum to calculate IRs for comparison to experimental data [21]. The best match value of 0.115 for the ^{79}Br^m/^{80}Br^m IR was achieved with the Back-shifted Fermi Gas Model [37] with a spin cut-off parameter multiplied by a factor of 0.1 [21], and the Simplified Modified Lorentzian Model [39]. The best match value of 0.330 for the ^{80}Br^m/^{80}Br^g IR, which agrees with values calculated in other work [46], was achieved with the Generalized Superfluid Model [40, 41] with a spin cut-off parameter multiplied by a factor of 0.2 [21], and the Gogny-Hartree-Fock-Bogoliubov model [42]. There is a disagreement between our experimentally observed IR of 0.211 and that reported by Pavalvanov et al. [46]; however, systematic factors, such as an overcalculation of the ^{80}Br^g population resulting from the more complex active target geometry, are removed when calculating double ratios between irradiation cases, as discussed later. Notably, the curtailed angular momentum distributions are in agreement with trends observed by Rodrigo et al. [38] in calculating isomeric ratios with TALYS following reactions with incoming massive particles. In our case, more sharply curtailed distributions may be representative of the limited angular momentum carried by incoming photons relative to massive particles.

Considering the exclusive $(\gamma/e^-, n)$ feeding of the ^{80}Br^m and ^{80}Br^g states, the associated IRs provide the clearest insight into the physical processes involved. Comparing the IRs by irradiation case in Table II indicates a factor of 4.354 ± 0.932 increase in the effective population of the isomeric state in ^{80}Br^g following irradiation by electron beams as compared to bremsstrahlung. FLUKA simulations comparing the stainless steel bremsstrahlung spectrum and internally generated LaBr$_3$ bremsstrahlung spectrum are plotted in Figure 3.
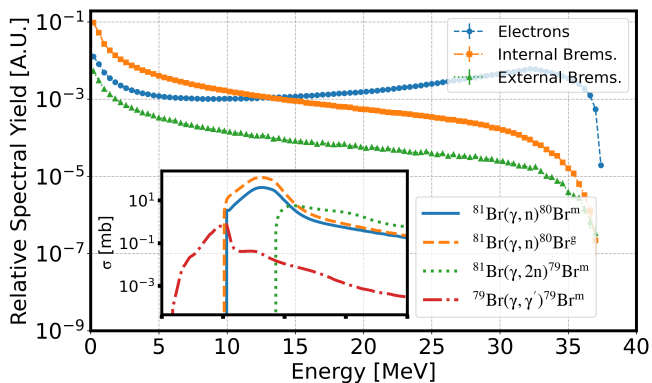
FIG. 3: Simulated spectra at the LaBr$_3$ active target comparing the internally generated bremsstrahlung (brems.) and electron scattering spectrum following direct electron irradiation with external brems. from the converter. Calculated with FLUKA for a flat distribution electron beam at 35 ± 2.5 MeV. The inset shows TALYS calculated microscopic cross sections from adjusted best fit parameters, with the x-axis depicting the same energy range as the larger plot.

The LaBr$_3$ internal bremsstrahlung spectrum was used to calculate an IR of 0.328 with identical TALYS parameters as given above, which indicates that the observed differences cannot be attributed to differences in photo-nuclear interactions.

Previous works have examined (e, e') excitation of isomeric states using few MeV electrons, but did not explore $(e, e'n)$ reactions [43, 44]. An experiment performed by Dzhilavyan et al. [45] compared the population of the $J^\pi = 12^-$, ^{196}Au^{m2} isomer following bremsstrahlung (γ, n) and $(e, e'n)$ reactions on ^{197}Au with $E_e = 59$ MeV, which indicated an $18 \pm 3\%$ increase in the population of the isomer relative to the $J^\pi = 2^-$, ^{196}Au^g state following electron bombardment. They suggest that enhanced population of the isomeric state following electron irradiation may be due to increased population of higher energy states, as compared to photons. Longer γ-cascades from these states could result in larger angular momentum transfer to the residual nucleus, with potential contributions from quasi-direct neutrons carrying additional angular momentum [45]. In contrast to Dzhilavyan et al., our enhancement is 18.64 ± 5.25. Further comparison of these results is difficult given the cumulative differences in nuclei, isomer-to-ground spin ratios, state parities, electron energies, and electron bunch duration.

CONCLUSIONS

This work demonstrates the ability to alter populations of long-lived isomeric states in ^{80}Br nuclei through excitation into the quasicontinuum using a compact laser-plasma accelerator. A factor of 4.354 ± 0.932 increase in the ^{80}Br^m/^{80}Br^g isomeric ratio following irradiation with fs electron beams as compared to photons indicates that further theoretical probing of nuclear-plasma interactions in the quasicontinuum should be explored. Studying quasicontinuum-localized NPIs in the presence of energetic, high-charge density fs electron beams is important for the further development of efficient isomer population manipulation techniques. Further experimental work will be performed.

Improved understanding of NPIs and electro-nuclear interactions could influence heavy element stellar nucleosynthesis through modifications to the angular momentum of residual nuclei. These results establish the utility of ultra-short pulse electron beams from laser-plasma accelerators as a novel platform for isomer manipulation and studies of statistical nuclear properties, such as γ-strength functions and nuclear level densities.

[1] Ward, R. The Importance of Long-Lived Isomeric States in s-Process Branching. *Astrophys. J..* **216**, 540-547 (September 1977)

[2] Busso, M., Gallino, R., & Wasserburg, G. Nucleosynthesis in Asymptotic Giant Branch Stars: Relevance for Galactic Enrichment and Solar System Formation. *Annual Review Of Astronomy And Astrophysics.* **37**, 239-309 (1999). https://doi.org/10.1146/annurev.astro.37.1.239

[3] Misch, G., Ghorui, S., Banerjee, P., Sun, Y., & Mumpower, M. Astromers: Nuclear Isomers in Astrophysics*. *The Astrophysical Journal Supplement Series.* **252**, 2 (December 2020). https://dx.doi.org/10.3847/1538-4365/abc41d

[4] Feng, J., Wang, W., Fu, C., Chen, L., Tan, J., Li, Y., Wang, J., Li, Y., Zhang, G., Ma, Y., & Zhang, J. Femtosecond Pumping of Nuclear Isomeric States by the Coulomb Collision of Ions with Quivering Electrons. *Phys. Rev. Lett..* **128**, 052501 (January 2022). https://link.aps.org/doi/10.1103/PhysRevLett.128.052501

[5] Guttormsen, M., Larsen, A. C., Midtbø, J. E., Crespo Campo, L., Görgen, A., Ingeberg, V. W., Renstrøm, T., Siem, S., Tveten, G. M., Zeiser, F., & Kirsch, L. E. Gamma-widths, lifetimes and fluctuations in the nuclear quasi-continuum. *EPJ Web Conf..* **178**, 06001 (2018). https://doi.org/10.1051/epjconf/201817806001

[6] Utsunomiya, H., Goriely, S., Kondo, T., Iwamoto, C., Akimune, H., Yamagata, T., Toyokawa, H., Harada, H., Kitatani, F., Lui, Y., Larsen, A., Guttormsen, M., Koehler, P., Hilaire, S., Péru, S., Martini, M., & Kon-

ing, A. Photoneutron cross sections for Mo isotopes: A step toward a unified understanding of (γ,n) and (n,γ) reactions. *Phys. Rev. C.* **88**, 015805 (July 2013). `https://link.aps.org/doi/10.1103/PhysRevC.88.015805`

[7] Tveten, G., Spyrou, A., Schwengner, R., Naqvi, F., Larsen, A., Eriksen, T., Bello Garrote, F., Bernstein, L., Bleuel, D., Crespo Campo, L., Guttormsen, M., Giacoppo, F., Görgen, A., Hagen, T., Hadynska-Klek, K., Klintefjord, M., Meyer, B., Nyhus, H., Renstrøm, T., Rose, S., Sahin, E., Siem, S., & Tornyi, T. Completing the nuclear reaction puzzle of the nucleosynthesis of ^{92}Mo. *Phys. Rev. C.* **94**, 025804 (August 2016). `https://link.aps.org/doi/10.1103/PhysRevC.94.025804`

[8] Chankova, R., Schiller, A., Agvaanluvsan, U., Algin, E., Bernstein, L., Guttormsen, M., Ingebretsen, F., Lönnroth, T., Messelt, S., Mitchell, G., Rekstad, J., Siem, S., Larsen, A., Voinov, A., & Ødegård, S. Level densities and thermodynamical quantities of heated $^{93\text{-}98}$Mo isotopes. *Phys. Rev. C.* **73**, 034311 (2006). `https://link.aps.org/doi/10.1103/PhysRevC.73.034311`

[9] Harston, M. & Chemin, J. Mechanisms of nuclear excitation in plasmas. *Phys. Rev. C.* **59**, 2462-2473 (1999). `https://link.aps.org/doi/10.1103/PhysRevC.59.2462`

[10] Gosselin, G., Méot, V. & Morel, P. Modified nuclear level lifetime in hot dense plasmas. *Phys. Rev. C.* **76**, 044611 (2007). `https://link.aps.org/doi/10.1103/PhysRevC.76.044611`

[11] Tkalya, E. Nuclear excitation in atomic transitions (NEET process analysis). *Nuclear Physics A.* **539**, 209-222 (1992). `https://www.sciencedirect.com/science/article/pii/037594749290267N`

[12] Morita, M. Nuclear Excitation by Electron Transition and Its Application to Uranium 235 Separation. *Progress Of Theoretical Physics.* **49**, 1574-1586 (1973). `https://doi.org/10.1143/PTP.49.1574`

[13] Cue, N., Poizat, J. & Remillieux, J. Exciting the Nucleus by Target Electron Capture into Atomic Orbitals. *Europhysics Letters.* **8**, 19 (1989). `https://dx.doi.org/10.1209/0295-5075/8/1/004`

[14] Esarey, E., Schroeder, C. & Leemans, W. Physics of laser-driven plasma-based electron accelerators. *Rev. Mod. Phys..* **81**, 1229-1285 (2009). `https://link.aps.org/doi/10.1103/RevModPhys.81.1229`

[15] Chen, Q., Jacob, R., Tilborg, J., Gonsalves, A., Nakamura, K., Schroeder, C., Esarey, E. & Geddes, C. Development of the MeV Thomson-scattered gamma ray source using laser plasma accelerators at the BELLA Center. *Compact Radiation Sources From EUV To Gamma-rays: Development And Applications.* PMorita1973582, PMorita19735820C (2023). `https://doi.org/10.1117/12.2665755`

[16] Tsai, H., Swanson, K., Barber, S., Lehe, R., Mao, H., Mittelberger, D., Steinke, S., Nakamura, K., Tilborg, J., Schroeder, C., Esarey, E., Geddes, C. & Leemans, W. Control of quasi-monoenergetic electron beams from laser-plasma accelerators with adjustable shock density profile. *Physics Of Plasmas.* **25**, 043107 (2018). `https://doi.org/10.1063/1.5023694`

[17] Elleaume, P., Chubar, O. & Chavanne, J. Computing 3D magnetic fields from insertion devices. *Proceedings Of The 1997 Particle Accelerator Conference (Cat. No.97CH36167).* **3**, 3509-3511 vol.3 (1997).

[18] Laeter, J., Böhlke, J., Bièvre, P., Hidaka, H., Peiser, H., Rosman, K. & Taylor, P. Atomic weights of the elements. Review 2000 (IUPAC Technical Report). *Pure And Applied Chemistry.* **75**, 683-800 (2003). `https://doi.org/10.1351/paRatkiewicz20180375060683`

[19] National Nuclear Data Center, B. NuDat (Nuclear Structure and Decay Data). (March 18, 2008).

[20] Ratkiewicz, A., Hopkins, L., Bleuel, D., Cassata, W., Cerjan, C., Dauffy, L., London, R., Meeker, D., Velsko, C., & Yeamans, C. Activation of enriched environmental xenon by 14-MeV neutrons. *Journal Of Radioanalytical And Nuclear Chemistry.* **317**, 169-175 (2018). `https://doi.org/10.1007/s10967-018-5911-4`

[21] Koning, A., Hilaire, S., & Duijvestijn, M. TALYS: Comprehensive Nuclear Reaction Modeling. *AIP Conference Proceedings.* **769**, 1154-1159 (May 2005). `https://doi.org/10.1063/1.1945212`

[22] Ahdida, C., Bozzato, D., Calzolari, D., Cerutti, F., Charitonidis, N., Cimmino, A., Coronetti, A., D'Alessandro, G., Donadon Servelle, A., Esposito, L., Froeschl, R., García Alía, R., Gerbershagen, A., Gilardoni, S., Horváth, D., Hugo, G., Infantino, A., Kouskoura, V., Lechner, A., Lefebvre, B., Lerner, G., Magistris, M., Manousos, A., Moryc, G., Ogallar Ruiz, F., Pozzi, F., Prelipcean, D., Roesler, S., Rossi, R., Sabaté Gilarte, M., Salvat Pujol, F., Schoofs, P., Stránský, V., Theis, C., Tsinganis, A., Versaci, R., Vlachoudis, V., Waets, A., & Widorski, M. New Capabilities of the FLUKA Multi-Purpose Code. *Frontiers In Physics.* **9** (2022). `https://www.frontiersin.org/articles/10.3389/fphy.2021.788253`

[23] Battistoni, G., Boehlen, T., Cerutti, F., Chin, P., Esposito, L., Fassò, A., Ferrari, A., Lechner, A., Empl, A., Mairani, A., Mereghetti, A., Ortega, P., Ranft, J., Roesler, S., Sala, P., Vlachoudis, V., & Smirnov, G. Overview of the FLUKA code. *Annals Of Nuclear Energy.* **82**, 10-18 (2015). `https://www.sciencedirect.com/science/article/pii/S0306454914005878`, Joint International Conference on Supercomputing in Nuclear Applications and Monte Carlo 2013, SNA + MC 2013. Pluri- and Trans-disciplinarity, Towards New Modeling and Numerical Simulation Paradigms

[24] Vlachoudis, V. Flair: A powerful but user friendly graphical interface for FLUKA. (2009). `https://cds.cern.ch/record/2749540`

[25] Kopecky, J., & Uhl, M. Test of gamma-ray strength functions in nuclear reaction model calculations. *Phys. Rev. C.* **41**, 1941-1955 (May 1990). `https://link.aps.org/doi/10.1103/PhysRevC.41.1941`

[26] Goriely, S., & Khan, E. Large-scale QRPA calculation of E1-strength and its impact on the neutron capture cross section. *Nuclear Physics A.* **706**, 217-232 (2002). `https://www.sciencedirect.com/science/article/pii/S0375947402008606`

[27] Brink, D.M. Individual particle and collective aspects of the nuclear photoeffect. *Nuclear Physics.* **4**, 215-220 (1957). `https://www.sciencedirect.com/science/article/pii/0029558287900216`

[28] Axel, Peter. Electric Dipole Ground-State Transition Width Strength Function and 7-Mev Photon Interactions. *Phys. Rev.* **126**, 671–683 (Apr 1962). `https://link.aps.org/doi/10.1103/PhysRev.126.671`

[29] Goriely, S., Samyn, M., & Pearson, J. Further explorations of Skyrme-Hartree-Fock-Bogoliubov mass formu-

las. VII. Simultaneous fits to masses and fission barriers. *Phys. Rev. C.* **75**, 064312 (June 2007). `https://link.aps.org/doi/10.1103/PhysRevC.75.064312`

[30] Goriely, S., Hilaire, S., & Koning, A. Improved microscopic nuclear level densities within the Hartree-Fock-Bogoliubov plus combinatorial method. *Phys. Rev. C.* **78**, 064307 (December 2008). `https://link.aps.org/doi/10.1103/PhysRevC.78.064307`

[31] Hilaire, S., Girod, M., Goriely, S., & Koning, A. Temperature-dependent combinatorial level densities with the D1M Gogny force. *Phys. Rev. C.* **86**, 064317 (December 2012). `https://link.aps.org/doi/10.1103/PhysRevC.86.064317`

[32] Chadwick, M., Herman, M., Obložinský, P., Dunn, M., Danon, Y., Kahler, A., Smith, D., Pritychenko, B., Arbanas, G., Arcilla, R., Brewer, R., Brown, D., Capote, R., Carlson, A., Cho, Y., Derrien, H., Guber, K., Hale, G., Hoblit, S., Holloway, S., Johnson, T., Kawano, T., Kiedrowski, B., Kim, H., Kunieda, S., Larson, N., Leal, L., Lestone, J., Little, R., McCutchan, E., MacFarlane, R., MacInnes, M., Mattoon, C., McKnight, R., Mughabghab, S., Nobre, G., Palmiotti, G., Palumbo, A., Pigni, M., Pronyaev, V., Sayer, R., Sonzogni, A., Summers, N., Talou, P., Thompson, I., Trkov, A., Vogt, R., Van der Marck, S., Wallner, A., White, M., Wiarda, D., & Young, P. ENDF/B-VII.1 Nuclear Data for Science and Technology: Cross Sections, Covariances, Fission Product Yields and Decay Data. *Nuclear Data Sheets.* **112**, 2887-2996 (2011). `https://www.sciencedirect.com/science/article/pii/S009037521100113X`, Special Issue on ENDF/B-VII.1 Library

[33] Singh, B. Nucl. Data Sheets 135, 193. (2016).

[34] Singh, B. Nucl. Data Sheets 105, 223. (2005).

[35] Farhan, A. R. and Singh, B. Nucl. Data Sheets 110, 1917. (2009).

[36] Jacob, R., Ostermayr, T., Tsai, H., Hakimi, S., Fan-Chiang, L., Barber, S., Isono, F., Van Tilborg, J., Gonsalves, A., Nakamura, K., Toth, C., Schroeder, C., Geddes, C., Esarey, E. & Lbnl Bella Team A hundred TW dual laser system for compact laser plasma accelerators, laser driven photon sources, and HED experiments at BELLA Center. *APS Division Of Plasma Physics Meeting Abstracts.* **2021** pp. eBO04.007 (2021,1)

[37] Dilg, W., Schantl, W., Vonach, H., & Uhl, M. Level density parameters for the back-shifted Fermi gas model in the mass range 40 ¡ A ¡ 250. *Nuclear Physics A*, **217**(2), 269-298 (1973). `https://doi.org/10.1016/0375-9474(73)90196-6`

[38] Rodrigo, A., Otuka, N., Takács, S., & Koning, A. J. Compilation of isomeric ratios of light particle induced nuclear reactions. *At. Data Nucl. Data Tables.* **153**, 101583 (2023). `https://doi.org/10.1016/j.adt.2023.101583`

[39] Goriely, S., Dimitriou, P., Wiedeking, M., Belgya, T., Firestone, R., Kopecky, J., Krtička, M., Plujko, V., Schwengner, R., Siem, S., Utsunomiya, H., Hilaire, S., Péru, S., Cho, Y. S., Filipescu, D. M., Iwamoto, N., Kawano, T., Varlamov, V., & Xu, R. Reference database for photon strength functions. *Eur. Phys. J. A.* **55**, 172 (October 2019). `https://doi.org/10.1140/epja/i2019-12840-1`

[40] Ignatyuk, A. V., Istekov, K. K., & Smirenkin, G. N. Collective effects in level density, and the probability of fission. *Sov. J. Nucl. Phys. (Engl. Transl.)* **30**, (November 1979). `https://www.osti.gov/biblio/5176754`

[41] Ignatyuk, A. V., Weil, J. L., Raman, S., & Kahane, S. Density of discrete levels in ^{116}Sn. *Phys. Rev. C.* **47**, 1504–1513 (April 1993). `https://doi.org/10.1103/PhysRevC.47.1504`

[42] Goriely, S., Hilaire, S., Péru, S., & Sieja, K. Gogny-HFB+QRPA dipole strength function and its application to radiative nucleon capture cross section. *Phys. Rev. C.* **98**, 014327 (July 2018). `https://doi.org/10.1103/PhysRevC.98.014327`

[43] Booth, E. C., & Brownson, J. Electron and photon excitation of nuclear isomers. *Nucl. Phys. A.* **98**, 529–541 (1967). `https://doi.org/10.1016/0375-9474(67)90097-8`

[44] Olariu, S., Olariu, A., Martin, D., & Niculescu, A. Search for γ-emission from isomeric nuclei induced by MeV electron beams. *Hyperfine Interact.* **135**, 71–81 (July 2001). `https://doi.org/10.1023/A:1013994507113`

[45] Dzhilavyan, L. Z., Lazareva, L. E., Ponomarev, V. N., & Sorokin, A. A. Isomeric ratios of the yields of the reactions ^{197}Au$(\gamma,$n$)^{196m}$,gAu and ^{197}Au(e,e'n)^{196m},gAu at energies 10–90 MeV. *Sov. J. Nucl. Phys.* **33**, 308–313 (1981). `http://inis.iaea.org/search/search.aspx?orig_q=RN:13701940`

[46] Palvanov, S. R., Egamova, F. R., Ramazanov, A. Kh., Palvanova, G. S., & Inoyatov, A. Kh. Excitation of isomeric states in the reactions $(\gamma,$ n) and (n, 2n) on the ^{81}Br nucleus. *Phys. Part. Nucl. Lett.* **18**, 672–675 (November 2021). `https://doi.org/10.1134/S1547477121060108`